While modification A is an improvement over the original method of Handlos and Baron, the absolute percentage deviation of 25 is still high. It is hoped that future work, both theoretical and experimental, will result in a more accurate description of the droplet mass transfer mechanism at high Reynolds numbers. For example, at very high N_{Re} when oscillation of droplet shape is encountered, it is rather doubtful that the circulation patterns as assumed in this model will actually be observed.

NOTATION

A_n = coefficients in Equation (2), dimensionless

a_i = coefficients in Equation (17), dimensionless; i = 0, 1, 2, 3, 4

B_n = coefficients in Equations (3) and (16), dimensionless

b = a constant defined by Equation (11)

C = concentration of solute in dispersed phase

C_o, C_f, C^* = initial, final, and equilibrium concentrations, respectively, (initial and final are uniform concentrations)

D_L, D_e = molecular diffusivity of the solute in the dispersed and continuous phase, respectively

D_{eff} = experimental effective mass diffusivity of the solute in droplet

d = droplet diameter

E_m = extraction efficiency during free fall period = $(C_o - C_f)/(C_o - C^*)$, dimensionless

$\overline{E}$ = effective diffusivity predicted by Equation (7)

h = modified continuous phase mass transfer coefficient, defined by Equation (13)

k_c, k_d = individual mass transfer coefficient, continuous and dispersed phase, respectively

K_d = overall mass transfer coefficient, dispersed phase, cm./sec.

K = variation constant defined by Equation (18), dimensionless

m = dispersed phase concentration/continuous phase concentration at equilibrium

$M(t)$ = mass of solute in dispersed phase at time t

n = an integer number

N_{Re} = droplet Reynolds number = $\frac{dU\rho_c}{\mu_c}$

$(N_{Sc})_c$ = continuous-phase Schmidt number = $\frac{\mu_c}{\rho_c D_c}$

r = $4\rho/d$ = torus radius, dimensionless

t = time during free fall period

$\overline{t}$ = average circulation time in droplet

t_c = approximate continuous film contact time = d/U

U = droplet free fall (or rise) velocity

y = $1 - r$ = distance in from surface of torus, dimensionless

$Y_n(y)$ = a function of y alone (eigenfunction)

$\overline{Z}$ = average displacement of fluid

Greek Letters

λ_n = an eigenvalue, dimensionless

μ_d, μ_c = viscosity of dispersed and continuous phase, respectively

ρ = torus radius

ρ_c = density of continuous phase

σ = interfacial tension

LITERATURE CITED

1. Calderbank, P. H., and I. J. O. Korchinski, *Chem. Eng. Sci.*, **6**, 65 (1956).
2. Elzinga, R. E., Jr., and J. T. Banchero, *Chem. Engr. Prog. Symposium Series No. 29*, **55**, 149 (1959).
3. Garner, F. H., and A. H. P. Skelland, *Ind. Eng. Chem.*, **46**, 1255 (1954).
4. ———, and M. Tayeban, *Anal. Real Sociedad Espanola Fisica y Quimica*, Series B, **LVI(B)**, 479 (1960).
5. Griffith, R. M., *Chem. Eng. Sci.*, **12**, 198 (1960).
6. Groeber, H., *Z. Ver. Deutsch Ing.*, **69**, 705 (1925).
7. Hadamard, J., *Compt. Rend.*, **152**, 1735 (1911).
8. Handlos, A. E., and T. Baron, *A.I.Ch.E. Journal*, **3**, 127 (1957).
9. Harriott, P., *Chem. Eng. Sci.*, **17**, 149 (1962).
10. Heertjes, P. E., W. A. Holve, and H. Talsma, *Chem. Eng. Sci.*, **3**, 122 (1954).
11. Higbie, R., *Trans. Am. Inst. Chem. Engrs.*, **31**, 365 (1935).
12. Johnson, A. I., and A. E. Hamislec, *A.I.Ch.E. Journal*, **6**, 145 (1960).
13. Kronig, R., and J. C. Brink, *Appl. Sci. Res.*, **A-2**, 142 (1950).
14. Lapidus, L., "Digital Computers for Chemical Engineers," p. 222, McGraw-Hill, New York (1962).
15. Linton, E., and K. L. Sutherland, *Chem. Eng. Sci.*, **12**, 214 (1960).
16. Newman, A. B., *Trans. Am. Inst. Chem. Engrs.*, **27**, 203 (1931).
17. Rybczinski, W., *Bull. Acad. Sci. Cracovie*, **A**, 40 (1911).
18. Treybal, R., "Liquid Extraction," p. 182, McGraw-Hill, New York (1963).
19. Weinstock, H., "Calculus of Variations," p. 241, McGraw-Hill, New York (1952).

Incipient Bubble Destruction and Particulate Fluidization

FREDERICK A. ZENZ

Squires International Inc., Roslyn Harbor, New York

On the basis of recent studies of single-particle drag and of bed-shearing forces in horizontal flow, a simple mechanism is proposed for the formation or destruction of bubbles in fluidized beds.

A MODEL OF INCIPIENT BUBBLE DESTRUCTION

Figure 1 schematically illustrates the well demonstrated flow patterns in and around a rising bubble (5). The interstitial fluidizing velocity field is designated by V_{mf}, the *shell* of dense bed surrounding the bubble, through which there exist the streams of recirculating fluid, is outlined by the dashed lines and its thickness designated by y; the horizontally directed surface velocity of the circulating fluid along the bottom of the bubble is denoted as U. Over the major portion of the bubble's lower surface there exists a velocity gradient penetrating the shell, which in terms of Figure 1 can be denoted by dU/dy. This velocity gradient creates a shearing stress tending to dilate the bed within the depth y. If this dilation is sufficient in magnitude to swell the bottom surface to within a few particle diameters of the upper surface then the bubble is destroyed or rather its incipient formation is thwarted. This is true, not only because it becomes "flooded" by the swelling bottom surface, but also because the upper surface particles will collapse onto the particles approaching from beneath when their distance of separation is small enough to disturb the drag forces on the upper particles (6).

To evaluate this mechanism of bubble formation, even if only qualitatively, requires means of calculating U, y, and the bed-dilating *dispersive grain pressures* resulting from dU/dy.

VELOCITY GRADIENT AND DISPERSIVE GRAIN PRESSURE

A rather unique measurement of what he chose to call dispersive grain pressures, a measure of bed dilation forces, was reported by R. A. Bagnold (2) in 1954. His apparatus consisted of a pair of concentric drums. The solid outer drum could be rotated at

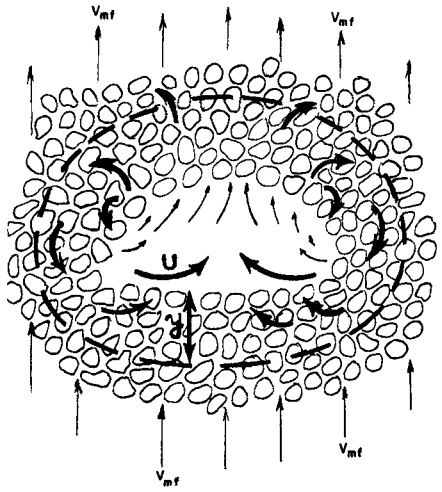

Fig. 1. Model of fluid velocity patterns in the area of influence of a bubble rising through a fluidized bed of particles.

various speeds. The periphery of the stationary inner drum was made of sheet rubber sealed to the drum flanges. The inside of the inner drum communicated through a hollow spindle with a manometer. Both the inner and outer drums were filled with water. On rotating the outer drum the manometer indicated the excess pressure in the annular space, exerted on the rubber sheathed inner drum, due to the centrifugal force on the rotating fluid between the drum flanges from the axis to the radius of the inner drum periphery. These pressures were recorded at various speeds of rotation. A measured volume of granular solids was then added to the annular space between the drums and again pressures were recorded at various speeds of rotation. The difference in recorded pressure with grains in the annular space and with plain fluid in the space was taken as representative of a so-called dispersive grain pressure. The grains used in these tests were spherical particles made of a nearly 50% mixture of paraffin wax and lead stearate with a very constant diameter of 0.132 cm. Their density differed from that of water by less than 0.1%.

Stated in the simplest terms, Bagnold measured the force on the wall of a container caused by the random impaction of particles against each other as they moved past the wall, all in the same net direction but at relatively different velocities. The velocity gradient in the annulus of his apparatus caused certain particles or layers of particles to move more rapidly than others. This means that some particles would catch up with others and bounce them aside. The process might be viewed as a multitude of continuous grazing billiard shots occurring within an incompressible fluid medium, or as random molecular collisions in an ideal gas where now drum rotational speed is replaced by temperature level. One might expect that in such an annular apparatus the resulting pressure would depend on the square of the speed of rotation, since doubling the speed would double the relative particle velocities and also double the frequency of impacts. This is in accord with Bagnold's results. He plotted dispersive grain pressure versus $\rho_P D_P^2 (dU/dy)^2$, which is proportional to (rpm) (2), giving lines of constant voidage, or solids concentration, which are straight and parallel with a slope of unity.

With Bagnold's results as a measure of the forces tending to dilate or disperse a bed of solids (subjected to the shearing force of a horizontal fluid velocity gradient), one needs to determine the value of dU/dy for the bubble model of Figure 1 in order to make some relative quantitative comparisons.

Harrison et al. (3) presented a theory defining the maximum stable bubble size in a powder maintained fluid by aeration at just the minimum fluidizing velocity. This bubble size is found by setting bubble velocity equal to the terminal velocity of an individual particle in free fall. Bubble diameter D_B is computed as the diameter of a sphere having a volume equal to the bubble, and is related to bubble velocity V_B by the expression $V_B = 0.711\sqrt{gD_B}$. Harrison et al. postulate that the intensity of gas circulation within a bubble is proportional to the bubble's velocity of rise. A large rapidly rising bubble may have such intense internal circulation that particles injected into it by whatever mechanism will be entrained by the circulating gas. These particles will therefore remain in the bubble, and the bubble will therefore tend to become smaller. A small bubble, on the other hand, will not have sufficient internal circulation to retain a particle injected into it. Thus they conclude that a stable maximum bubble size must exist, and that the factors which determine its size are the intensity of internal circulation and the settling velocity of an individual particle in free fall. They also cite the work of Bagnold (1) on horizontal transport velocity of small particles as an indication that perhaps the terminal free-fall velocity might not be the relevant parameter for computing bubble sizes in beds of very fine particles.

Squires (8) illustrated the magnitude of bubble sizes calculated by the theory of Harrison et al. for typical fluid-particle systems in which bubble characteristics have been observed and reported by many investigators. His results showed that the calculated bubble sizes for particle sizes below about 0.01 in. are certainly much below observed sizes. Squires proposed that in place of terminal velocity one might more realistically assume that single particle saltation velocity would apply, since the particles would be entrained in the bubble void by the recirculating gas flow sweeping across the particle surface making up the bottom of the bubble. Bubble sizes recalculated on this assumption showed excellent agreement with observations. Thus one can conclude that in an existing bubble the horizontal sweeping gas velocity designated by U in Figure 1 must at least be approximated by single particle saltation velocities, V_{s_o}, for which correlations have been proposed (10).

The question of how deep an internal circulating gas flow might penetrate into the shell of dense phase powder surrounding the bubble void can be answered to a good first approximation from the experiments of Wace and Burnett (9) and the theoretical studies of Rowe (5). Wace and Burnett observed the gas flow in a *two-dimensional* bed fluidized with air. By admitting dark brown nitrogen dioxide through small holes drilled into the face wall of the bed near the grid plate, they were able to observe the gas flow streamlines up through the bed and through the bubbles. Rowe drew an analogy of their results to the ideal case of two- and three-dimensional flow through a body of infinite extent containing a circular hole. In the two-dimensional case all the fluid in a zone having a width of two radii on either side of the center line through the hole (or bubble) passed through the hole so that the velocity therein was twice that of the remote fluid. In the three-dimensional case the gas velocity in the spherical void was three times that in the remote fluid (where the remote fluid was analogous to the dense particle mass in the fluidized bed). This means that gas is drawn from a shell of thickness equal to $D_B(\sqrt{3} - 1)/2$ surrounding the bubble.

DISPERSIVE PRESSURE WITHIN A BUBBLE

From the work of Rowe and Squires a first approximation of the velocity gradient within the bottom surface of a bubble can simply be shown proportional to V_{s_o} and D_B in the form

$$\frac{dU}{dy} \sim \frac{V_{s_o}}{D_B(\sqrt{3}-1)/2} \qquad (1)$$

From the work of Harrison et al.

$$D_B = \left(\frac{V_B}{0.711\sqrt{g}}\right)^2 \qquad (2)$$

and since Squires has shown that to a better approximation V_B is proportional to V_{s_0} one can write

$$D_B \sim \frac{V_{s_0}^2}{(4.03)^2} \qquad (3)$$

so that

$$\frac{dU}{dy} \sim \frac{1}{V_{s_0}} \text{ and } \left(\frac{dU}{dy}\right)^2 \sim \left(\frac{1}{V_{s_0}}\right)^2 \qquad (4)$$

The dispersive grain pressure measurements of Bagnold have as a correlant the square of velocity gradient which is thus proportional to $1/V_{s_0}^2$.

The theoretical stable bubble sizes calculated by Squires can now be compared with the magnitude of the velocity gradient, or rather the dispersive pressure. A high velocity gradient corresponds to a high dispersive pressure and certainly a high dispersive pressure coupled with a small theoretically stable bubble size would lead to bubble disappearance or at any rate small probability of bubble formation ever fully occurring.

From correlations (*10*) of V_{s_0} it is possible to calculate relative values of the gradient $(dU/dy)^2$ within the bubble as a function of particle diameter. The results of such calculations are shown in Figure 2 for a few typical systems. Since Bagnold showed dispersive pressure to be directly proportional to velocity gradient, the ordinate

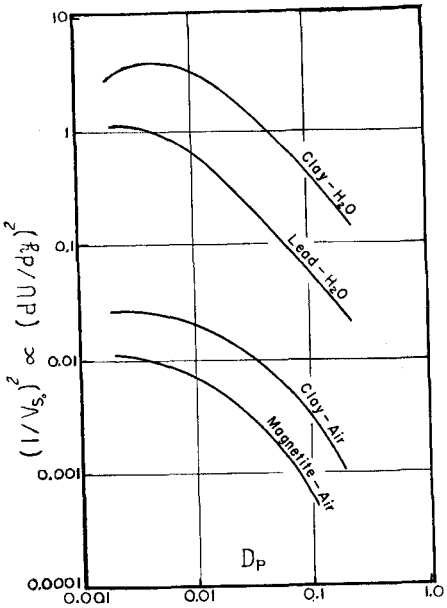

Fig. 2. Velocity gradients or dispersive pressures for various fluid-particle systems.

of Figure 2 could be relabelled P_G; however, Bagnold showed that dispersive pressure is also a function of voidage. Since the loosest static bed density of powders is a function of particle size (finer powders exhibiting high bulk voidages), the curves of Figure 2 can be corrected for voidage. In making this correction it is assumed that the curves of Figure 2 are based on 40% voids for all particle sizes and that the actual voidage is a function of particle size as given in several sources (*11*). This voidage correction to Figure 2 bends the curves downward to a greater and greater extent as particle diameter decreases and effectively flattens them to the results shown in Figure 3 in which the ordinate is now labelled P_G. The degree of displacement due to the voidage correction is illustrated for the clay-water system in Figure 3 by the dashed curve, which is taken from Figure 2. Unfortunately, there is no direct quantitative means for matching the P_G scale to the abscissa. Quantitatively the coordinates of Figure 3 are reasonable and probably near the proper magnitude since Bagnold's measurements went up to 2 lb./sq. ft. at a voidage of 40%.

The ordinate of Figure 3 is a measure of the force tending to dilate the solids making up the bottom surface of the largest calculable stable bubble in a fluidized bed of particles of the size given in the abscissa. Since the gradient and, hence, dispersive, pressure is related to a calculated maximum bubble size, it is not to be implied that bubbles will or do exist under all conditions, but merely that if they did exist they would have a dis-

(*Continued on page 573*)

Kinetics of Ethane Pyrolysis

JOHN R. BARTLIT and HARDING BLISS

Yale University, New Haven, Connecticut

In the course of the development of a flow reactor for the study of pyrolysis reactions some interesting observations about the method and results with ethane have been determined. The essence of this method is the rapid mixing of ethane with very hot nitrogen at a temperature below that required for pyrolysis in an attempt to reduce the large axial temperature gradients usually experienced in a flow reactor. During the course of this work others (*1*) have arrived at a related idea and have developed the scheme with considerable success. The nature of the data and the treatment thereof vary considerably in the two cases.

Ethane was pyrolyzed at 696 to 826°C. and one atmosphere for contact times of 0.21 to 2.2 sec. with 9 to 72% decomposition. The ethane content of the mixed stream varied from 7 to 22%.

John R. Bartlit is at the University of California, Los Alamos, Scientific Laboratory, Los Alamos, New Mexico.

EXPERIMENTAL

Apparatus

The preheater-reactor (see Figure 1) was a Vitreosil quartz tube 7 mm. O.D. x 5 mm. I.D., in the shape of a tee with a cross near one end of the horizontal. The horizontal member was 31¼ in. long and the vertical 18 in. The vertical member was used for preheating ethane. The first 18 in. of the horizontal member was used for preheating nitrogen, the next 8¼ in. for the reaction zone proper, and the last 5 in. (which were outside the insulating box) for the admission of a thermocouple. The outlet cross was made of two 1 in. lengths of the same tubing to admit cold nitrogen as a quench and to discharge the products. In normal operation, the quench and discharge were through these short 2 in. lengths and the straight section of the quartz tube was plugged with a rubber *policeman*. When a gas temperature traverse was made, the straight section was unplugged and the gases allowed to flow out of this straight section.

The ethane leg was heated by means of 30 ft. of B & S 20 g. Nichrome wire on 15¾ in. (four units) of Norton Alundum grooved cores (No. 9099) and embedded in Norton RA 1162 cement. The nitrogen leg was heated by means of 24 ft. of 0.032 in. diameter Baker No. 1 platinum wire, similarly wound. The reaction zone was heated by means of 17¼ ft. of B & S 20 g. Kanthal A-1 resistance wire wound into a tight coil on a mandrel and stretched to allow about 1/16 in. between turns. This heater was held in place on the reaction tube with the same Alundum cement. The other heaters were, of course, removable. Certain thermocouples were immersed in this cement. Each of the three heaters was con-

(*Continued on following page*)

(Continued from page 562)

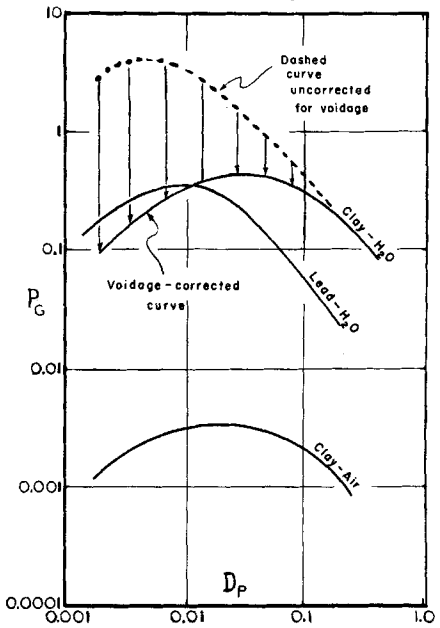

Fig. 3. Dispersive pressure curves of Figure 2 corrected for particle size effect on voidage.

persive pressure within their bottom surface of the magnitude given in Figure 3.

The existence of a dispersive pressure begs the question as to why it doesn't simply exert its influence and dilate the solids to the eventual destruction of any bubble. Since this does not happen in all cases, it is obvious that the magnitude of the dispersive pressure must be compared with the magnitude of whatever force it must move against to effect the dispersion. The first force against which the dispersive pressure must act is the weight of the uppermost layer of particles on the bottom surface of the bubble. The weight of this layer is simply $\rho_P(1-\epsilon)D_P/12$ in units of lb./sq. ft. if ρ_P is expressed in lb./cu. ft. and D_P in inches. The voidage ϵ is again taken from published sources (*11*) corresponding therefore to the conditions on which the curves of Figure 3 are based. Figure 4 is a reproduction of Figure 3 with curves of $\rho_P(1-\epsilon)D_P/12$ corresponding to clay catalyst and lead shot superimposed.

Note in Figure 4 that for the water-clay catalyst system the dispersive pressure curve intersects the single-particle-layer weight curve and that to the left of this intersection the dispersive pressure exceeds the layer weight.

To the left of this point of intersection the beds should dilate and no bubbles will be able to persist, whereas in beds of larger particle size the dispersive pressure cannot overcome the particle weight; hence bubbles will persist. Note that in accord with reported

(Continued on following page)

ERRATA

Equation (1*d*) of the article "Problem of Solidification with Newton's Cooling at the Surface" by Peter Hrycak (Vol. 9, No. 4, pp. 585-589) should read

$$-k_1\frac{\partial T_1}{\partial x} = -k_2\frac{\partial T_2}{\partial x} - \frac{d\xi}{dt}L, \qquad x=\xi$$

In the paper "On Stress-Relaxing Solids: Part III, Simple Harmonic Deformation" by Saul Vela, J. W. Kalb, and A. G. Fredrickson (Vol. 11, No. 2, pp. 288-294), Equation (14) should read

$$\Psi(\omega) = \int_0^\infty e^{-i\omega t}\,\psi(t)\,dt$$

The first line of Equation (19) should read

$$\Psi(\omega) = \int_0^\infty e^{-i\omega t}\,\psi(t)\,dt$$

In the paper "Mass Transfer in Horizontally Moving Stable Aqueous Foams" by Eugene Y. Weissman and Seymour Calvert (Vol. 11, No. 2, pp. 356-363), the first footnote on page 359 should begin with the term N_{tp}.

(Continued from page 572)

A study of perfectly mixed photochemical reactors, Harris, Paul R., and Joshua S. Dranoff, **A.I.Ch.E. Journal, 11,** No. 3, p. 497 (May, 1965).

Key Words: A. Decomposition-8, Hexachloroplatinic Acid-1, Water-5, Performance-8, Reactor-9, 8, Photochemical-0, Perfect Mixing-10, Absorption Coefficients-8, Design-8, Scale-Up-8, Hydrochloric Acid-2, Ultraviolet Light-10, Radius-6, Reaction Rate-7, 8. B. Mathematical Analysis-8, Quantum Efficiency-10, Lambert's Law-10, Reactor-9, Photochemical-0.

Abstract: The performance of a perfectly mixed photochemical reactor has been analyzed mathematically for systems having low light absorption coefficients. The analysis has been tested by an experimental study of the decomposition of hexachloroplatinic acid in dilute aqueous solution. Results tend to verify the analysis, but indicate the need for additional experimental work.

Heat transfer characteristics of boiling nitrogen and neon in narrow annuli, Lapin, Abraham, H. C. Totten, and L. A. Wenzel, **A.I.Ch.E. Journal, 11,** No. 3, p. 503 (May, 1965).

Key Words: A. Boiling-8, Heat Transfer-8, 9, Nitrogen-2, Neon-2, Submergence-6, Difference-6, Temperature-9, 6, Roughness-6, Surface-9, 6, Heat Flux-7, Copper-10, Nickel-10, Cadmium-10, Annuli-9, 6, Narrow-0, Gap-9, 6, Cryogenic Fluids-5, Cylinder-10, Nucleate Boiling-8, Vertical-0, Condenser-10, Heater-10, Metals-10, Correlation-8, Dittus-Boelter Equation-10.

Abstract: The boiling characteristics of liquid and nitrogen in vertical annuli ranging between 0.006 and 0.080 in. wide were studied. The center tube wall, submerged to various depths, formed the boiling surface. Observations suggested a convective equation form proved successful.

Determination of the activity coefficient of a volatile component in a binary system by gas-liquid chromatography, Chueh, Chun F., and Waldemar T. Ziegler, **A.I.Ch.E. Journal, 11,** No. 3, p. 508 (May, 1965).

Key Words: A. Activity Coefficient-8, 9, Vapor-Liquid Equilibria-8, 9, Phase Equilibria-8, 9, Equilibrium-8, 9, Measurement-8, Gas-Liquid Chromatography-10, 8, Binary System-9, Retention Volume-8, 7, Concentration-6, Temperature-6. B. Activity Coefficient-8, Benzene-1, Diethylene Glycol-5, Aromatic Compounds-1, Hydrocarbons-1, Alcohols-5, Glycols-5, Experimental-0. C. Activity Coefficient-8, *n*-Hexane-1, Trichlorobenzene-5, Hydrocarbons-1, Aliphatic Compounds-1, Alkanes-1, Chlorinated Hydrocarbons-5, Halogenated Hydrocarbons-5, Experimental-0.

Abstract: The gas-liquid chromatographic method of measuring the activity coefficient of the solute in a binary system was extended from infinite dilution to finite concentration range. An equation expressing the retention volume is presented. Experimental results of two binary systems were compared with those obtained by the static equilibrium method.

Influence of catalyst particle size on reaction kinetics: hydrogenation of ethylene on nickel, Fulton, J. W., and O. K. Crosser, **A.I.Ch.E. Journal, 11,** No. 3, p. 513 (May, 1965).

Key Words: Ethylene-0, Hydrogen-1, Ethane-2, Nickel-4, Diluent Particles-0, Packed Bed-5, Flow Rate-0, Particle Size-6, Heat Transfer-0, Mass Transfer-0, Thermal Regime-7, Catalysis-0, Film Diffusion-0, Heterogeneous Reaction-0, Hydrogenation-0, *j*-Factor-0, Reaction Kinetics-8, Pore Diffusion-9, Reaction-10.

Abstract: The influence of catalyst particle size upon the reaction rate was studied for the hydrogenation of ethylene with nickel-on-alumina in a packed-bed flow reactor. A threefold increase in particle diameter through a critical size range (0.03- to 0.09-cm. diameter, corresponding to a Reynolds number of around 1) produced a thirtyfold increase in reaction rate per unit external surface area. The behavior of the system indicates that this increase was due to the influence of external gas-solid transport phenomena on the reaction kinetics. *j*-Factor correlations were used to calculate the catalyst surface temperatures and concentrations, which were used to calculate Arrhenius activation energies and reaction rates from available rate expressions.

(Continued on page 576)

(Continued from preceding page)

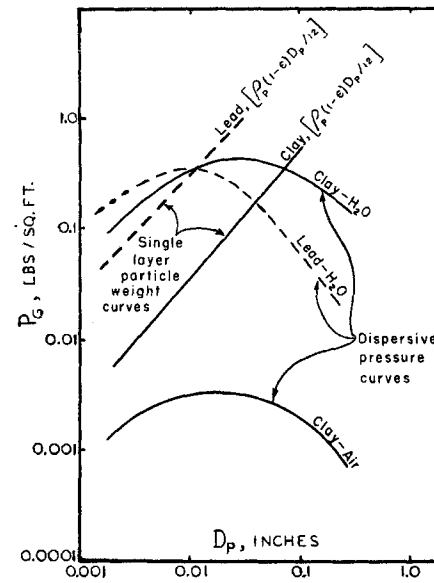

Fig. 4. Relative magnitude of dispersive pressure and weight of a single layer of particles.

observations the air-clay system dispersive pressure is always below the particle-layer weight curve and thus this system always exhibits bubbles, whereas in water medium only very large clay catalyst particles will allow bubbles to persist. Also in accord with reported observations, lead particles would exhibit bubbles in water medium for all but the very smallest particle sizes.

The above reasoning would appear plausible only for a point condition and raises the question of what happens in beds of small particle size after the solids have dilated (and thereby thwarted the bubble), since then the bed exhibits a higher voidage and hence a lower dispersive pressure. However, if the voidage increases, the particle layer weight also decreases. This raises the question of which decreases more rapidly with increased voidage: the particle layer weight or the dispersive pressure? As illustrated schematically in Figure 5 for a bed of constant particle size exhibiting no bubbles at an incipient fluidization voidage of ϵ_i the bed may expand without distinct bubbles to a voidage of approximately ϵ_4, at which point its unit layer weight will equal the dispersive pressure. Further expansion would be accompanied by bubble formation because the dispersive pressure could no longer counteract the weight of the bottom surface of a forming bubble. The change in dispersive pressure with voidage is again obtainable from Bagnold's results and the particle layer weight from the expression $\rho_P(1-\epsilon)D_P/12$. Such particulate (nonbubble) fluidization to bed expansions of rather high voidage prior to the observation

(Continued on following page)

(Continued from preceding page)

of distinct bubbles have been reported by Simpson and Rodger (7) who carried out extensive experiments with light solids fluidized in dense pressured gases as well as heavy solids fluidized in water.

There are also systems in which particulate fluidization is observable over the entire range of voidages from the static bed to a single suspended particle. Bagnold's results would ordinarily indicate such rapid decrease in P_g with increased voidage that the particle layer weight curve would always be passed (as illustrated in Figure 5) well before ϵ neared 1.0, the value for expansion to the single suspended particle. However, the possibility of bubble formation is overcome as soon as bed expansion has reached the point where particles are far enough apart so that the wake behind one particle will not touch or sufficiently influence the flow field facing the next nearest downstream particle to cause it to fall down onto its upstream neighbor (*12*). Once the particles are that far apart there is also no longer a mechanism for stabilizing the roof of the bubble and thus the entire question of bubbles vanishes. If, as illustrated in Figure 5, the particle separation at ϵ_4 or at lower voidages already exceeds wake length, then the bed will expand further to $\epsilon = 1.0$ without bubble formation, even if the dispersive pressure is zero. Observations of dilute phase fluidization, even for systems exhibiting violent bubbling at low voidages, are in accord with this viewpoint. Further work on the influence of neighboring particles on drag, such as reported on

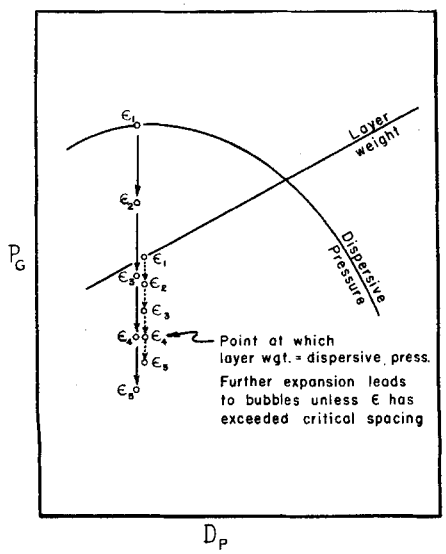

Fig. 5. Schematic illustration of change in dispersive pressure and particle layer weight with bed expansion during fluidization.

(Continued on following page)

INFORMATION RETRIEVAL

(*Continued from page 574*)

Forced convection mass transfer: Part I. Effect of turbulence level on mass transfer through boundary layers with a small favorable pressure gradient, Thomas, David G., **A.I.Ch.E. Journal, 11,** No. 3, p. 520 (May, 1965).

Key Words: A. Mass Transfer-8, 7, Turbulence-6, Convection-7, Forced-0, Boundary Layers-9, Laminar-0, Turbulent-0, Napthalene-5, Hydrocarbons-5, Air-5, Wind Tunnel-10, Velocity-6, Flow-9.

Abstract: The effect of free stream turbulence level on forced convection through laminar and turbulent boundary layers on a flat plate was studied in a wind tunnel with a small but nonzero favorable pressure gradient by means of the naphthalene sublimation technique. The rate of mass transfer was determined by measuring the level of a naphthalene surface before and after exposure in the wind tunnel.

The viscosity of nonpolar gas mixtures at moderate and high pressures, Dean, David E., and Leonard I. Stiel, **A.I.Ch.E. Journal, 11,** No. 3, p. 526 (May, 1965).

Key Words: A. Calculation-8, Viscosity-9, 8, 7, Gases-9, Mixtures-9, Nonpolar-0, Molecular Weights-10, Physical Properties-10, 9, 8, 7, Critical Constants-10, Pressure-6, Comparison-8, Mathematical-0, Experimental-0.

Abstract: A method has been developed for the calculation of the viscosity of nonpolar gas mixtures at moderate and elevated pressures from the molecular weights and critical constants of the components. By the use of available experimental data and appropriate pseudocritical constant rules, results obtained previously for the viscosity of pure gases have been extended to mixtures. Viscosity values calculated by the method developed in this study for a number of nonpolar gas mixtures were found to reproduce reported values with a high degree of accuracy.

An analytical solution for the nonlinear frequency response of radiant heat transfer, Blum, Edward H., **A.I.Ch.E. Journal, 11,** No. 3, p. 532 (May, 1965).

Key Words: A. Frequency Response-8, Nonlinear-0, Heat Transfer-9, 8, Radiation-10, Conduction-10, Perturbation Analysis-10, Oscillatory Frequency-6, Physical Properties-6, Phase Angle-7, Amplitude-7, Temperature-8, Ricatti Differential Equation-10.

Abstract: An analytical solution is presented for the nonlinear frequency response of a system in which radiant heat transfer is coupled with conduction. The model is that of an object inside an evacuated enclosure whose wall temperature oscillates about a mena. A perturbation analysis solves the describing equations for oscillatory amplitudes less than one-tenth the mean wall temperature. An exact solution to a Ricatti differential equation verifies the perturbation analysis. These solutions show that, contrary to linear experience, the average object temperature over an oscillatory cycle exceeds the mean at the wall.

Turbulence effect on direct-contact heat transfer with change of phase: effect of mixing on heat transfer between an evaporating volatile liquid in direct contact with an immiscible liquid medium, Sideman, Samuel, and Zvi Barsky, **A.I.Ch.E. Journal, 11,** No. 3, p. 539 (May, 1965).

Key Words: A. Correlation-8, Mixing-9, 8, 6, Heat Transfer-9, 8, 7, Evaporation-9, 6, Liquid-9, Theoretical-0, Experimental-0, Input-9, 7, Power-9, Water-9, Temperature-9, Pilot Plant-0, Laboratory-0, Pentane-9, Mixing Cell-10, Aliphatic Compounds-9, Alkanes-9, Hydrocarbons-9.

Abstract: Effect of mixing on heat transfer between an evaporating volatile liquid in direct contact with an immiscible liquid medium was studied theoretically and experimentally. Specific power input, temperature driving force, and heat flow rates are related for all conceivable mixing regimes. Pentane and water were used in the experiments.

(*Continued from preceding page*)

by Rowe, should help in establishing the critical particle separation.

The mechanisms proposed here as leading to natural destruction, or persistence, of bubbles suggest a broad spectrum of experimentation to provide the necessary tools for a quantitative treatment. A few selected systems chosen specifically to explore the region around the intersection of dispersive pressure and single layer weight curves have been observed (*4*) to be in accord with curves such as shown in Figures 4 and 5.

NOTATION

D_B = bubble diameter
D_P = particle diameter
g = gravitational constant
P_G = dispersion grain pressure
u = horizontally directed surface velocity of the circulating fluidizing medium along the inside bottom of the bubble
V_B = velocity of bubble rise through a fluidized bed
V_{s_o} = minimum horizontal fluid velocity required to prevent a particle from settling out along the bottom of a horizontal line
V_{mf} = superficial fluidization velocity
y = thickness of recirculating gas shell surrounding a bubble
ϵ = void fraction
ρ_P = particle density

LITERATURE CITED

1. Bagnold, R. A., "The Physics of Blown Sand and Desert Dunes," pp. 88-89, Methuen & Co., London, England (1941).
2. ———, *Proc. Royal Soc.*, **A225,** 49-63 (1954).
3. Harrison, D., J. F. Davidson, J. W. DeKock, *Trans. Inst. Chem. Engrs., (London),* **39,** 39 (1961).
4. Jakovac, J., M.S. thesis, Polytechnic Inst. Brooklyn (1966).
5. Rowe, P. N., *Chem. Engr. Progr. Symposium Series No. 38,* **58,** 42-56 (1962).
6. ———, and G. A. Heywood, *Trans. Inst. Chem. Engrs. (London),* **39,** 43 (1961).
7. Simpson, H. C., B. W. Rodger, *Chem. Engr. Sci.,* **16,** 153-180 (1961).
8. Squires, A. M., *Chem. Engr. Progr. Symposium Series No. 38,* **58,** 57-64 (1962).
9. Wace, P. F., S. J. Burnett, *Trans. Inst. Chem. Engrs. (London),* **39,** 168 (1961).
10. Zenz, F. A., "Modern Chemical Engineering," A. Acrivos, Ed., Chap. 6, Reinhold, New York (1963); also *I.E.C. Fundamentals,* **3,** 65-73 (1964).
11. ———, and D. F. Othmer, "Fluidization and Fluid-Particle Systems," p. 234, Reinhold, New York (1960).
12. *Ibid.*, pp. 257-258.